Transthyretin Cardiac Amyloidosis: A Noninvasive Multimodality Approach to Diagnosis Using Transthoracic Echocardiography, 99m-Tc-Labeled Phosphate Bone Scanning, and Cardiac Magnetic Resonance Imaging

Akhil Shukla, MB BCh, BSci, David Wong, MBBS, RANZACR, Julie A. Humphries, MBBS, BHMS(Ed), FRACP, FCSANZ, FASE, Benjamin T. Fitzgerald, MBBS, FRACP, Katrina Newbigin, MBBS, RANZACR, John Bashford, MBBS, FRACP, and Gregory M. Scalia, MBBS, MMedSci, FRACP, FCSANZ, FACC, FASE, *Brisbane, Australia*

INTRODUCTION

This case report highlights the utility of noninvasive imagining modalities, specifically transthoracic echocardiography in conjunction with nuclear medicine bone scan and cardiac magnetic resonance imaging (MRI) for the diagnosis of transthyretin (TTR) cardiac amyloidosis. Historically, the differentiation of this diagnosis from amyloid light chain (AL) amyloidosis is made via invasive endomyocardial biopsy, which has the risks of an invasive procedure, is limited by sampling errors, and does not provide information about the extent of involvement of different organs.[1] This case demonstrates a noninvasive approach to the differentiation of these two clinically distinct forms of amyloid.

CASE PRESENTATION

A 77-year-old man with a long-standing history of polyarthritis consulted his musculoskeletal physician for investigation of worsening neck and shoulder discomfort. As part of his workup, a Tc99m-hydroxymethylene diphoshonate (HDP) bone scan with single photon emission computed tomography (CT) imaging of the upper spine and delayed whole-body imaging demonstrated arthropathy of the cervical spine and shoulder girdle (see Figure 1A). Unexpectedly, this bone scan also demonstrated moderately increased, diffuse tracer uptake throughout the myocardium of the left ventricle (see Figure 1B).

This man had a background of hypertension controlled by a single antihypertensive agent as well as gout. He had no neuropathy, bowel symptoms, orthostatic hypotension, or visible periorbital or tongue infiltration. He had moderate exertional dyspnea (New York Heart Association class 2) and mild peripheral edema but clear lungs. His electrocardiogram did not show the classical low voltages of AL cardiac amyloidosis but rather demonstrated significant conduction disease with first-degree atrioventricular block, leftward axis, and a right bundle branch block (see Figure 1C). He had previously undergone a CT coronary angiogram, which demonstrated only minor coronary artery plaque.

Transthoracic echocardiography demonstrated moderately increased left ventricular wall thickness (septum, 17 mm; posterior wall, 15 mm; mass index, 142 g/m^2) and right ventricular thickness (13 mm), consistent with an infiltrative process (see Figure 2A and 2B, Videos 1-5). There was evidence of elevated left ventricular filling pressures (American Society of Echocardiography 2016 guidelines[2]) with mitral E/A = 0.75, E = 70 cm/sec, average E/e′ = 15, and left atrial volume index 35 mL/m^2. There was no pulmonary hypertension (right ventricular systolic pressure = 20 mm Hg) and normal transpulmonary gradient as indicated by an echocardiographic pulmonary to left atrial ratio of 0.14 m/sec.[3] Myocardial strain imaging of the left ventricle demonstrated a mild reduction in global longitudinal strain at −18.8%. Importantly, the polar map demonstrated the typical apical sparing pattern, which has become pathognomonic of cardiac amyloidosis[4] (see Figure 2C).

Cardiac MRI, with its unique ability to define myocardial infiltration and enhancement, was performed to supplement the echocardiogram. A 3 T scanner (Skyra, Siemens, Erlangen Germany) was used to acquire CINE views of the whole heart. Functional parameters were acquired by means of ARGUS analytical Software (Siemens, Germany). T1 mapping was performed pre- and 5 minutes postcontrast (0.2 mmol/kg of gadolinium), as early-phase postcontrast timing has the greatest point of discrimination in the setting of amyloidosis (see Videos 5 and 6).[5] There was increased left ventricular myocardial wall thickening (mean, 17 mm) and increased myocardial mass (145 g/m^2), which would be consistent with both light chain (AL) and TTR amyloidosis. There was excellent correlation of the left ventricular mass and wall thickness with the echocardiographically derived data. On T1 mapping, extracellular volume indices were supportive of a diagnosis of amyloidosis (see Figure 2D and 2E) with diffuse, predominantly transmural enhancement.

The usual workup for patients with the anatomic and functional features of cardiac amyloidosis focuses on first ruling in or ruling out the marrow diseases, multiple myeloma, and AL amyloidosis (see Figure 3).[6] In this patient, serum immunofixation electrophoresis studies excluded monoclonal paraproteinemia and urine immunofixation electrophoresis studies showed no suggestion of Bence-Jones protein. Bone marrow aspirate showed no clonal abnormality or immunoproliferative disorder. Abdominal wall fat pad biopsy showed

From the Wesley Hospital (A.S., B.T.F., J.B., G.M.S.); Wesley Medical Imaging (D.W., K.N.); Heart Care Partners (J.A.H., B.T.F., G.M.S.); ICON Cancer Care (J.B.); and the University of Queensland (G.M.S.), Brisbane, Australia.

Keywords: Amyloidosis, Echocardiography, Bone scan, Cardiac magnetic resonance imaging

Conflicts of Interest: The authors reported no actual or potential conflicts of interest relative to this document.

2468-6441

http://dx.doi.org/10.1016/j.case.2017.01.012

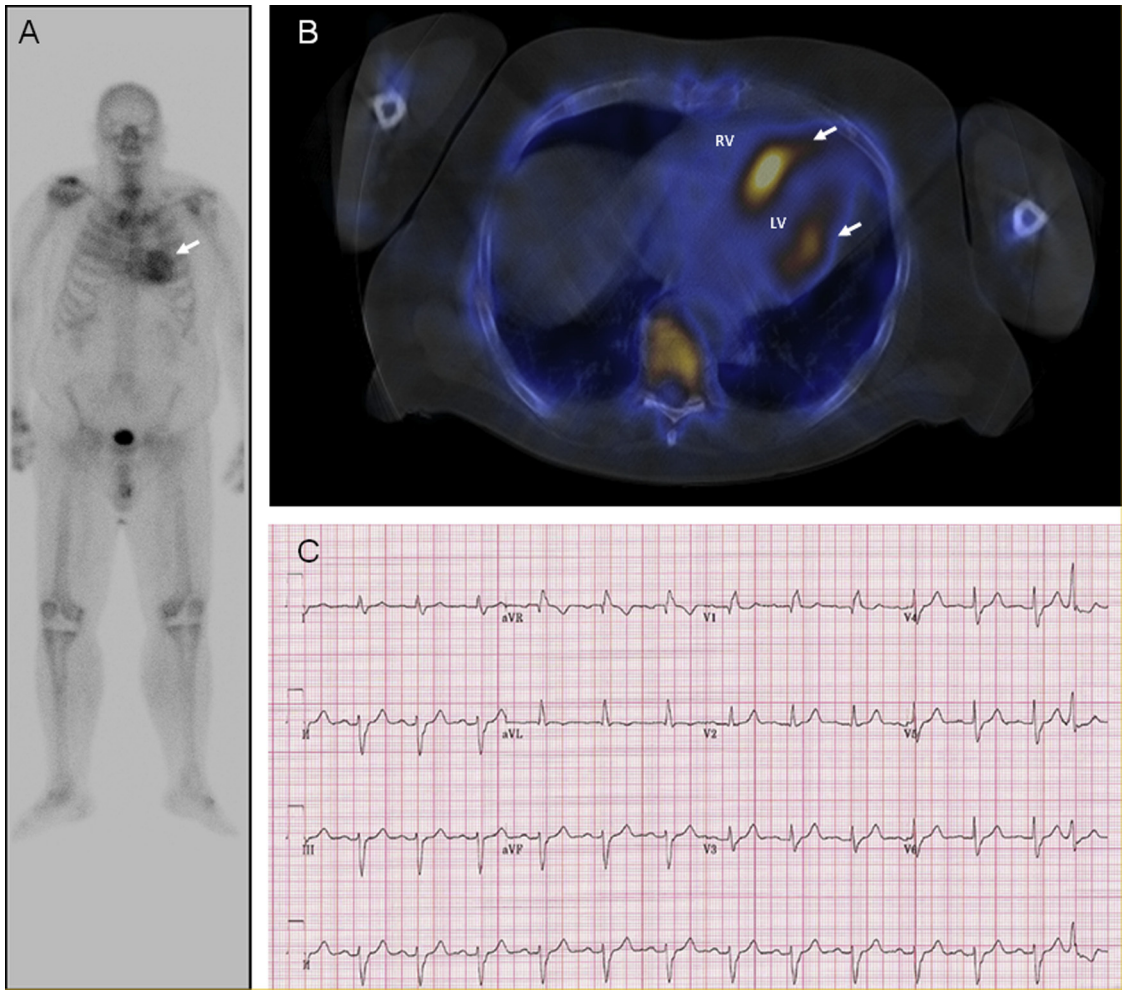

Figure 1 **(A)** Tc99m-HDP whole-body bone scan with single photon emission CT imaging demonstrating diffusely increased tracer uptake throughout the myocardium (*arrow*) and the right shoulder. **(B)** Axial tomographic scan, as viewed from the feet, of Tc99m-HDP bone scan tracer (*yellow*) in the walls (*arrows*) of the left ventricle (LV; RV, right ventricle). **(C)** Twelve-lead electrocardiogram did not show the classical low voltages of AL cardiac amyloidosis but rather showed significant conduction disease with first-degree atrioventricular block, leftward axis, and a right bundle branch block.

no morphological features of amyloid deposition. However, rectal biopsy was positive on congo-red stain, indicative of submucosal amyloid. Genetic testing was declined by the patient. With the provisional diagnosis of TTR cardiac amyloidosis, conservative management was chosen by the patient. Six-month follow-up repeat transthoracic echocardiography showed no progression of disease. The clinical status remained stable.

DISCUSSION

Amyloidosis results from extracellular deposition of insoluble fibrillary protein. Clinical manifestations of these diseases are myriad and depend on the various organ and tissue infiltrates in any given patient.[7] The nature of the unique protein in each case determines the pattern of organ involvement including nephropathy, polyneuropathy, ophthalmopathy, and cardiomyopathy. The classification of subtypes of amyloidosis is based on the source of production of the protein and includes the following.

- AL amyloid—plasma cell disorders, including multiple myeloma, with production of amyloid-forming monoclonal immunoglobulin (e.g., light chains). Cardiac involvement occurs in about 50% of cases. Prognosis is poor, with survival reported as 48 months, dropping to 5-8 months with cardiac involvement.[8]
- TTR—127 amino acid tetramer protein (formerly known as prealbumin) produced in the liver.[9]
  - Age-related (senile/wild-type) systemic amyloidosis is a sporadic, nongenetic disease misaggregation of a wild-type TTR monomer in the myocardium and other sites (gastrointestinal tract 25%). Untreated survival is measured in years to decades.
  - Mutant TTR amyloidosis—typically familial/autosomal dominant with peripheral and/or autonomic neuropathy and cardiomyopathy.[1]
- AA amyloid (chronic inflammation, serum amyloid A)—rarely results in cardiac involvement.
- Dialysis-related amyloidosis.
- Organ-specific amyloidosis.
- Heritable amyloidosis.

Cardiac amyloidosis is a progressive disorder beginning with subclinical myocardial deposition of fibrils, left and right ventricular wall thickening, and impairment of diastolic function.[10] As the volume of infiltration increases, patients develop clinical heart failure with preserved ejection fraction. Finally, end-stage cardiac amyloidosis involves systolic and diastolic dysfunction, cardiac conduction defects, and arrhythmias.[11]

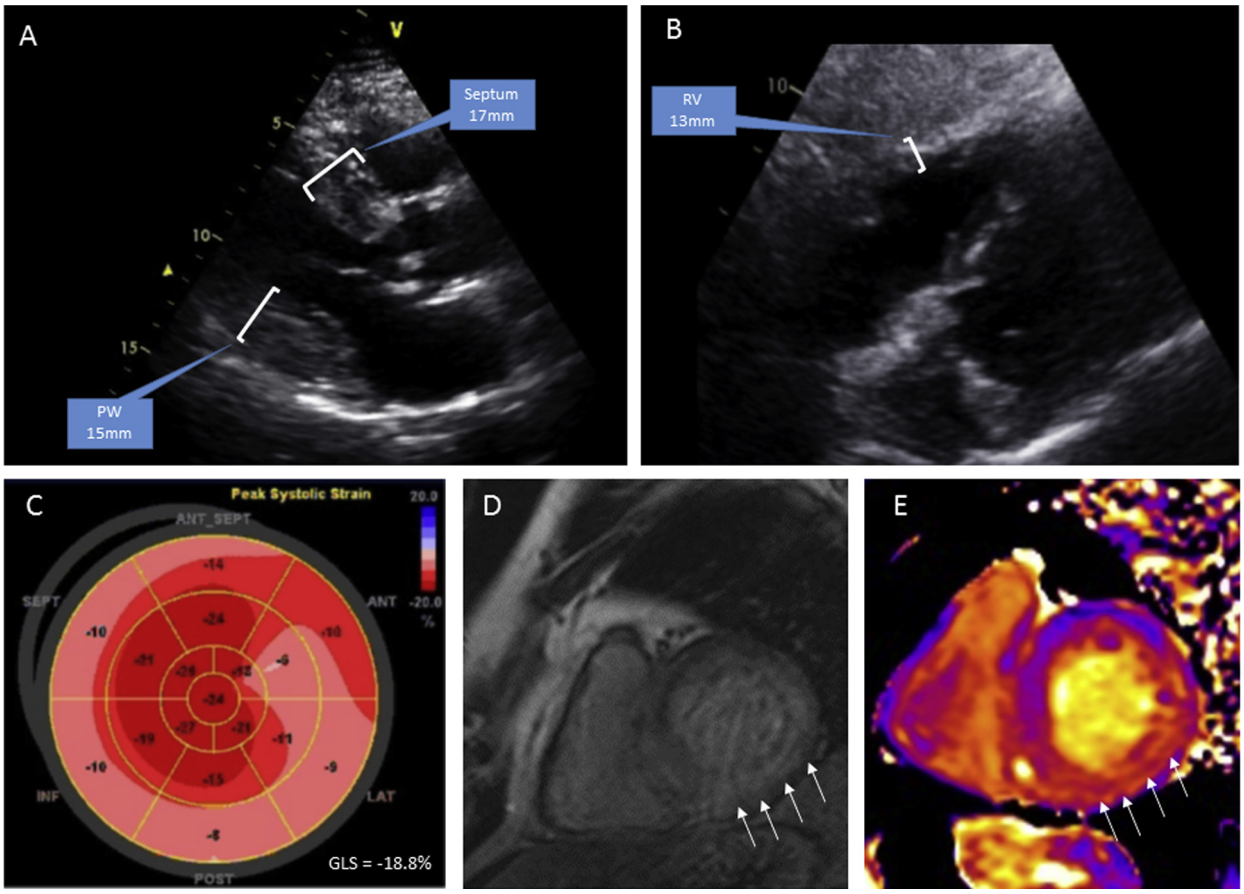

Figure 2 **(A)** Transthoracic echocardiographic parasternal long-axis view showing increased left ventricular posterior wall (PW) thickness of 15 mm and septal thickness of 17 mm. **(B)** Right ventricular (RV) free wall thickness increased at 13 mm on the subcostal view. **(C)** Apical longitudinal strain map with low normal global longitudinal strain (−18.8%) with classical "apical-sparing" pattern characteristic of cardiac amyloidosis. **(D)** Diffuse delayed myocardial gadolinium enhancement of the left ventricular myocardium (*arrows*). **(E)** Elevated native T1 values (indicated by the colors *red* and *orange*, *arrows*) suggesting diffuse amyloidosis with high extracellular water/protein volume.

Echocardiography has long been considered the cornerstone for the evaluation and management of patients with known or suspected cardiac amyloidosis.[12] This patient demonstrated the typical early findings of the disease, with impaired diastolic function and raised ventricular filling pressures. There was a mild reduction in global longitudinal peak systolic strain with apical sparing and impaired longitudinal contraction at the base—"bull's eye plot." This decrease in strain occurs before alterations in conventional echocardiographic parameters or the onset of symptomatic heart failure.[13,14] This strain pattern facilitates differentiation of cardiac amyloidosis from left ventricular hypertrophy and hypertrophic cardiomyopathy.[4]

This case highlights the potential use of echocardiography in conjunction with 99mTc-HDP bone scan as potential noninvasive early diagnostic tools for TTR cardiac amyloidosis.[14-16] Recent case reports with radiolabeled phosphate derivatives 99mTc-HDP[17] and 99mTc- methylene diphosphomate bone scans[18] have been shown to localize cardiac TTR amyloidosis. Radiolabeled 99mTc-3,3-diphosphono-1,2-propanodicarboxylic acid (DPD) has been reported to show approaching 100% discrimination in small studies.[19] The tracers 99mTc- pyrophosphate and 99mTc-DPD have been limited by technique, incomplete characterization of amyloid type, and inability to differentiate amyloidosis from other forms of cardiac failure.[19]

Semiquantitative MRI assessment of amyloid infiltration with T1 mapping has been validated to reflect the burden of cardiac amyloidosis disease.[20,21] Increasing extracellular volume reflects progressive edema and protein infiltration within the myocardial interstitial space. Extracellular volume has been associated with an increased mortality in light chain amyloidosis.[22] Serial T1 mapping can therefore be used in amyloidosis to monitor both disease progression and response to therapies.[23] In comparison with AL amyloidosis, TTR amyloidosis usually demonstrates lower native T1 values consistent with lower extracellular volume burden of disease.[24] In this case, elevated native T1 values of 1,450 (3T normal range, 1,100-1,150) and reduced post-contrast T1 of 220 (normal < 440) suggested a moderately high burden of disease, correlating with high uptake on bone scan.[25]

The treatment of cardiac amyloidosis is two-fold—manage the heart failure and manage the infiltrative process. Volume status is managed with loop diuretics and aldosterone antagonists. Beta-blockers may worsen heart failure in those for whom cardiac output is dependent on heart rate. While there are no clinical trials assessing the efficacy of angiotensin-converting enzyme inhibitors and angiotensin receptor blockers therapy in cardiac amyloidosis patients, clinical experience suggests that these agents often induce profound hypotension. Calcium channel blockers are ineffective in heart failure with

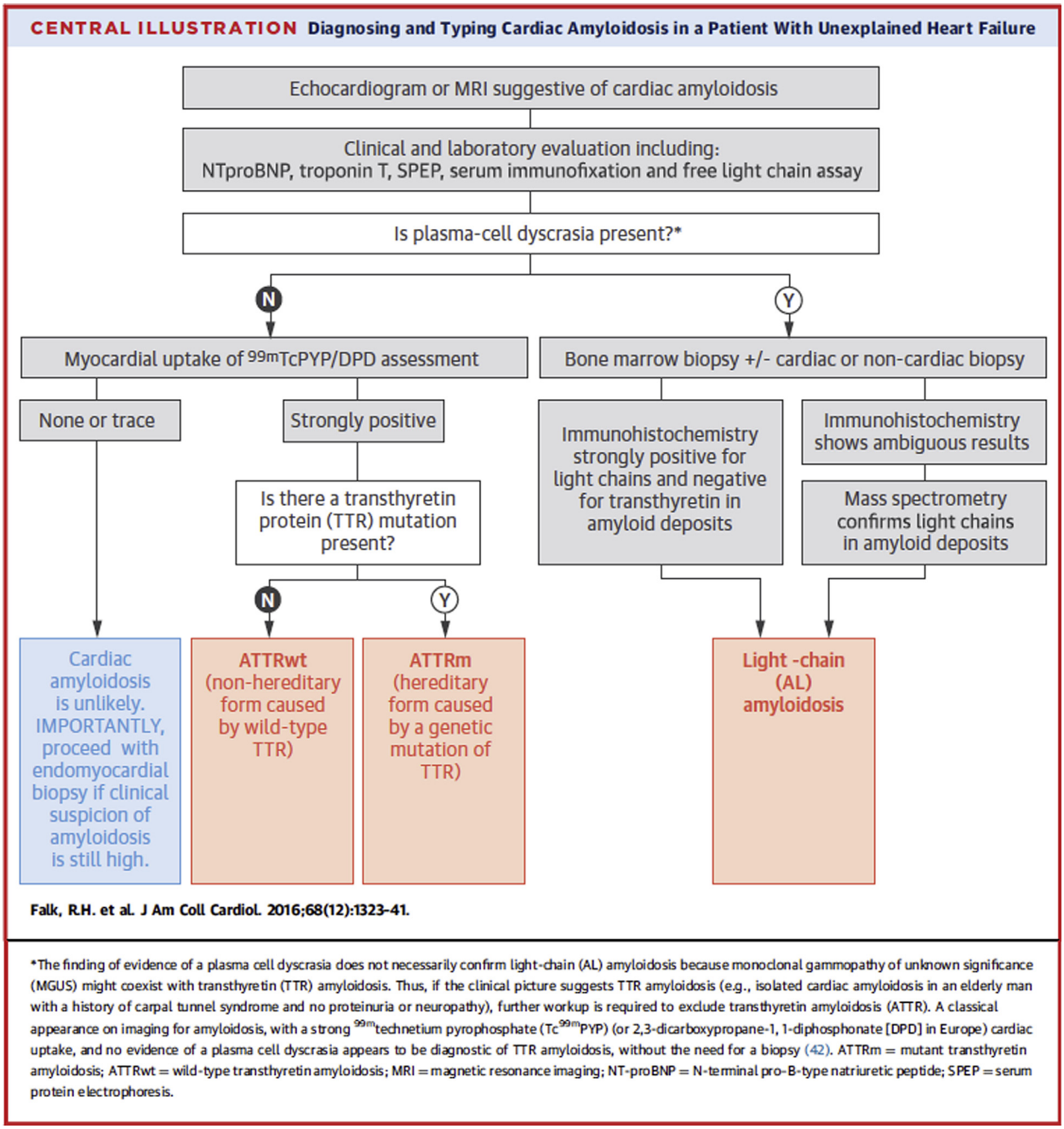

Figure 3 Schema for the workup of cardiac amyloidosis. The fundamental determination is whether a marrow illness (multiple myeloma/AL amyloid-plasma cell dyscrasias) is present. If not, the use of Tc99 m bone scan imaging is used to diagnose TTR amyloidosis (wild type or genetic). Reproduced with permission from Falk et al.[6]

preserved ejection fraction (diastolic heart failure) and are contraindicated due to their negative inotropic effects.[16]

Treatment of the underlying disease (e.g., control of plasma cell dyscrasia/myeloma) has dramatically changed the prognosis in AL amyloidosis.[8] The liver is the source of the abnormal protein in TTR amyloidosis. Patients with mutant/familial TTR cardiac amyloidosis have been treated with combined liver and heart transplant.[16] In senile systemic amyloidosis, the precursor protein is native (wild-type) TTR. Clinical trials are underway that involve potentially disease-modifying agents including TTR tetramer stabilizers (e.g., diflunisal), RNA inhibitors, and amyloid-degrading agents (e.g., doxycycline). Anti-SAP antibodies show promise in wild-type TTR amyloidosis, but clear indications and the toxicity profiles are still subject to clinical trials.[16]

CONCLUSION

Transthoracic echocardiography in conjunction with cardiac MRI is an essential component of a noninvasive multimodality approach to the diagnosis of cardiac amyloidosis of all origins. The affinity of 99m-Tc-labeled phosphate derivative bone scan tracer for TTR-associated cardiac amyloidosis directs the diagnosis away from

the marrow-related AL amyloidosis illnesses. Challenges exist in the identification of the early stages of this disease, however, these three imaging modalities demonstrate promise in this patient population.

SUPPLEMENTARY DATA

Supplementary data related to this article can be found at http://dx.doi.org/10.1016/j.case.2017.01.012.

REFERENCES

1. Noordzij W, Glaudemans A, Slart R, Dierckx R, Hazenberg B. Clinical use of differential nuclear medicine modalities in patients with ATTR amyloidosis. Amyloid 2012;19:208-11.
2. Nagueh S, Smiseth O, Appleton C, Byrd B, Dokainish H, Edvardsen T, et al. Recommendations for the evaluation of left ventricular diastolic function by echocardiography: An update from the american society of echocardiography and the european association of cardiovascular imaging. J Am Soc Echocardiogr 2016;29:277-314.
3. Scalia GM, Scalia IG, Kierle R, Beaumont R, Cross DB, Feenstra J, et al. ePLAR—The echocardiographic Pulmonary to Left Atrial Ratio—A novel non-invasive parameter to differentiate pre-capillary and post-capillary pulmonary hypertension. Int Jour of Card 2016;212:379-86.
4. Phelan D, Collier P, Thavendiranathan P, Popović ZB, Hanna M, Plana JC, et al. Relative apical sparing of longitudinal strain using two-dimensional speckle-tracking echocardiography is both sensitive and specific for the diagnosis of cardiac amyloidosis. Heart 2012;98(9):1442-8.
5. Cooper MA, Nguyen T, Maurer M, Landau H, Kim J, Gojraty S, et al. Early post-contrast T1 mapping yields maximal discriminatory capacity for detection of cardiac amyloid—influence of temporal T1 differences on MOLLI imaging. J Cardiovasc Magn Reson 2014;16(Suppl 1):322.
6. Falk RH, Alexander KM, Liao R, Dorbala S. AL (light-chain) cardiac amyloidosis: a review of diagnosis and therapy. JACC 2016;68:1323-41.
7. Falk RH, Comenzo RL, Skinner M. The systemic amyloidoses. N Engl J Med 1997;337:898-909.
8. Fitzgerald BT, Bashford J, Scalia GM. The return of the normal heart: Resolution of cardiac amyloidosis after chemotherapy and bone marrow transplantation. Heart Lung Circ 2013;22:655-60.
9. Ruberg FL, Berk JL. Transthyretin (TTR) cardiac amyloidosis. Circulation 2012;126:1286-300.
10. Falk RH. Cardiac amyloidosis—a treatable disease, often overlooked. Circulation 2011;124:1079-85.
11. Banypersad SM, Moon JC, Whelan C, Hawkins PN, Wechalekar AD. Updates in cardiac amyloidosis: a review. J Am Heart Assoc 2012;1:e000364.
12. Fitzgerald BT, Scalia GM, Cain PA, Garcia MJ, Thomas JD. Left atrial size—Another differentiator for cardiac amyloidosis. Heart Lung Circ 2011;20:574-8.
13. Di Bella G, Minutoli F, Piaggi P, Casale M, Mazzeo A, Zito C, et al. Quantitative comparison between amyloid deposition detected by 99mTc-Diphosphonate imaging and myocardial deformation evaluated by strain echocardiography in transthyretin-related cardiac amyloidosis. Circ J 2016;80:1998-2003.
14. Quintana-Quezada R, Yusuf S, Banchs J. Use of noninvasive imaging in cardiac amyloidosis. Curr Treat Options Cardio Med 2016;18:46.
15. Castano A, Bokhari S, Brannagan T III, Wynn J, Maurer M. Technetium pyrophosphate myocardial uptake and peripheral neuropathy in a rare variant of familial transthyretin (TTR) amyloidosis (Ser23Asn): a case report and literature review. Amyloid 2012;19:41-6.
16. Patel K, Hawkins P. Cardiac amyloidosis: where are we today? J Intern Med 2015;278:126-44.
17. Okayama S, Sugimoto M, Nakano T, Onoue K, Sakaguchi Y, Uemura S, et al. Cardiac amyloidosis incidentally detected using technetium-99m hydroxymethylene diphosphonate bone scintigraphy in a patient with prostate cancer. IJC Heart & Vessels 2014;4:213-4.
18. Yang L, Groth JV, Emmadi R. Cardiac amyloidosis detected on Tc-99m bone scan. Nucl Med Mol Imaging 2015;49:78-80.
19. Bokhari S, Shahzad R, Castano A, Maurer MS. Nuclear imaging modalities for cardiac amyloidosis. J Nucl Cardiol 2014;21:175-84.
20. Karamitsos TD, Piechnik SK, Banypersad SM, Fontana M, Ntusi NB, Ferreira VM, et al. Noncontrast T1 mapping for the diagnosis of cardiac amyloidosis. JACC Cardiovasc Imaging 2013;6:488-97.
21. Robbers LF, Baars EN, Brouwer WP, Beek AM, Hofman MBM, Niessen HWM, et al. T1 mapping shows increased extracellular matrix size in the myocardium due to amyloid depositions. Circ Cardiovasc Imaging 2012;5:423-6.
22. Banypersad SM, Fontana M, Maestrini V, Sado DM, Captur G, Petrie A, et al. T1 mapping and survival in systemic light-chain amyloidosis. Eur Heart J 2015;36:244-51.
23. Hur DJ, Dicks DL, Huber S, Mojibian HR, Meadows JL, Seropian SE, et al. Serial native T1 mapping to monitor cardiac response to treatment in light-chain amyloidosis. Circ Cardiovasc Imaging 2016;9.
24. Fontana M, Banypersad SM, Treibel TA, Maestrini V, Sado DM, White SK, et al. Native T1 mapping in transthyretin amyloidosis. JACC Cardiovasc Imaging 2014;7:157-65.
25. Dabir D, Child N, Kalra A, Rogers T, Gebker R, Jabbour A, et al. Reference values for healthy human myocardium using a T1 mapping methodology: results from the International T1 Multicenter cardiovascular magnetic resonance study. J Cardiovasc Magn Reson 2014;16:69.